Photoluminescence imaging of silicon wafers

T. Trupke[a)] and R. A. Bardos
*Centre of Excellence for Advanced Silicon Photovoltaics and Photonics, University of New South Wales,
Sydney 2052, Australia*

M. C. Schubert and W. Warta
Fraunhofer Institute for Solar Energy Systems, Heidenhofstrasse 2, D-79110 Freiburg, Germany

Photoluminescence imaging is demonstrated to be an extremely fast spatially resolved characterization technique for large silicon wafers. The spatial variation of the effective minority carrier lifetime is measured without being affected by minority carrier trapping or by excess carriers in space charge regions, effects that lead to experimental artifacts in other techniques. Photoluminescence imaging is contactless and can therefore be used for process monitoring before and after individual processing stages, for example, in photovoltaics research. Photoluminescence imaging is also demonstrated to be fast enough to be used as an in-line tool for spatially resolved characterization in an industrial environment. © *2006 American Institute of Physics.*
[DOI: 10.1063/1.2234747]

The characterization of silicon wafers by quasi-steady-state photoluminescence (QSS-PL) has recently been demonstrated to be very sensitive at small excess carrier concentrations, with excess carrier concentrations as small as 10^9 cm^{-3} detectable.[1] QSS-PL is unaffected by the so-called depletion region modulation (DRM) effect[1–3] and unaffected by minority carrier trapping in all practical cases,[4] effects that lead to artifacts in other lifetime techniques such as quasi-steady-state photoconductance (PC).[5] It has also been argued that QSS-PL is less sensitive to temperature variations upon illumination than other techniques.[6] The possibility of reliably detecting extremely small excess carrier concentrations from QSS-PL, in turn, allows implied current-voltage curves to be measured on silicon wafers over a very wide range of voltages in so-called Suns-photoluminescence experiments.[7] In the above cited work a large area PL sensor measured the material properties spatially averaged over an area of 2 $\times 2$ cm^2. With the current trend in photovoltaics of using cheaper and generally more defective silicon, in particular, multicrystalline silicon (mc-Si), there is, however, also a need for monitoring spatially resolved material properties. Mapping techniques such as PL mapping yield spatially resolved information about the material quality, e.g., about dislocation distributions[8] or about the local diffusion length.[9] Mapping is, however, generally time consuming and carried out with very large local illumination intensities equivalent to up to several thousands of Suns and cannot therefore be used for fast characterization of wafers under illumination intensities equivalent to 1 Sun. Several imaging methods based, for exemple, on free carrier infrared absorption[10,11] or on free carrier infrared emission[12] have been demonstrated over the last few years. In general, those techniques are subject to the same experimental artifacts at low carrier densities as spatially averaged PC measurements, i.e., artifacts resulting from minority carrier trapping[13] or from the DRM effect. The effect of minority carrier trapping can be suppressed to a large extent by continuous sub-band-gap illumination as demonstrated recently for the carrier density imaging technique.[14]

Given the sensitivity of QSS-PL and its robustness against artifacts, an imaging technique based on luminescence is ideal for the characterization of silicon wafers. Electroluminescence (EL) imaging of fully processed *silicon solar cells* has recently been demonstrated.[15,16] We present PL imaging of *silicon wafers*, which in comparison to EL imaging has the major advantages that it is contactless, does not require a device structure, and can therefore be applied to silicon wafers at any processing stage, allowing the influence of individual processing steps on the local material properties to be monitored.

A 15 W/815 nm diode laser was used to illuminate samples of up to 8.5×8.5 cm^2 with intensity variations $<5\%$ across that area. A commercially available one megapixel silicon charge-coupled device (CCD) camera (thermoelectrically cooled to -20 °C) in combination with a standard 28 mm lens from a 35 mm film camera was used for detection of the PL signal. Images could be recorded with variable laser power, with variable integration time and with signal detection from either the illuminated side or from the opposite surface. In this work illumination and detection of the PL signal are from the same side of the sample. Laser light that is reflected off the sample surface is blocked with a 1000 nm long pass filter (Schott glass RG1000) located between the sample and the CCD camera, which prevents incident laser light from contributing to the measured PL intensity. Absolute incident light intensities were measured with a calibrated silicon sensor.

Figure 1 shows a calibrated PL image taken on an 8.5×8.5 cm^2 large section from a 10×10 cm^2, 302 μm thick, 1.2 Ω m, mc-Si, *p*-type wafer with a SiN passivation layer deposited after chemical polishing. The incident photon flux was 2.5×10^{17} cm^{-2} s^{-1} corresponding to an electrical current density of $\sim$40 mA cm^{-2}, i.e., to about 1 Sun illumination. The total data acquisition time for that measurement was 1.5 s and the spatial resolution is 130 μm.

In Fig. 1 the relative pixel count was converted into a local effective minority carrier lifetime τ_{eff} using

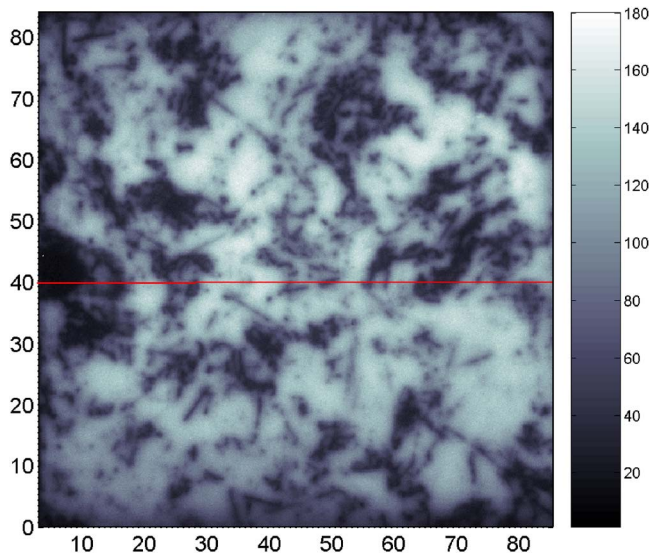[a)]FAX: +61-2-9662-4240; electronic mail: thorsten@trupke.de

FIG. 1. (Color online) Lifetime distribution within an 8.5×8.5 cm^2 area of a 302 μm thick, 1.2 Ω cm, mc-Si, *p*-type wafer obtained from a PL image measured with a data acquisition time of 1.5 s and with a spatial resolution of 130 μm.

$$\tau_{\text{eff}} = \frac{\Delta n}{G}. \tag{1}$$

The generation rate per unit volume G is calculated from the incident photon flux, the front surface reflectance, and the thickness of the wafer. The conversion of counts per pixel into a local excess carrier concentration Δn was achieved by comparison with the spatially averaged QSS-PL lifetime measurement taken at the same light intensity with a large area *P-I-N* detector in a 2×2 cm^2 area in the center of the wafer.

For comparison, Fig. 2 shows the spatially resolved minority carrier lifetime determined from an independently calibrated carrier density imaging (CDI) absorption measurement on the same wafer. A 939 nm semiconductor laser with a photon flux of 2.33×10^{17} cm^{-2} s^{-1} was used for excitation,
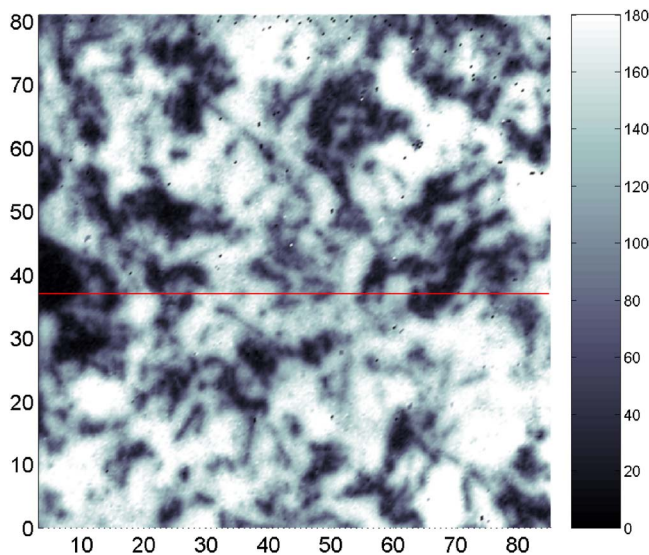

FIG. 2. (Color online) Lifetime distribution of the wafer from Fig. 1 measured with the carrier density imaging technique in absorption mode. Data acquisition time is 30 s and spatial resolution is 350 μm. The red line indicates the position of the line scan shown in Fig. 3.
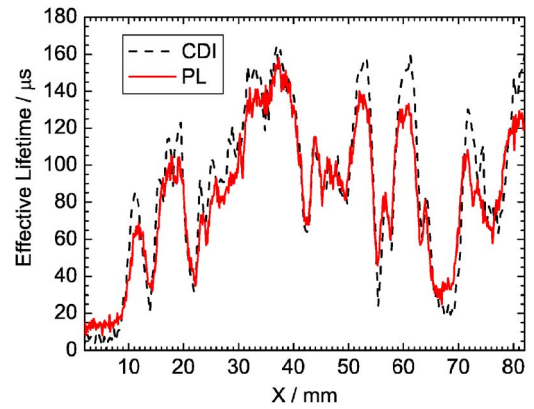

FIG. 3. (Color online) Effective lifetime from PL and from carrier density imaging (CDI) along the line marked in Figs. 1 and 2.

which is comparable to the measurement conditions of the PL measurement. The data acquisition time for the CDI measurement was 30 s and the spatial resolution is 350 μm. By comparing two CDI measurements with and without sub-band-gap bias light illumination,[14] we confirmed that minority carrier trapping has a negligible influence on the CDI results at this light intensity. Excellent quantitative and qualitative agreement is observed between the PL image and the CDI image, which is also highlighted by the comparison of two cross sections along the same line through the PL and CDI images, respectively, as shown in Fig. 3.

Valuable information about the influence of individual processing steps on the local material quality can also be gained from qualitative PL images. As an example for such qualitative process monitoring Fig. 4 shows two PL images of a 3.4×3.4 cm^2 section of a SiN passivated monocrystalline *p*-type 1 Ω cm silicon wafer with phosphorus diffusion on the front ($\sim$100 Ω/δ) and on the rear ($\sim$200–300 Ω/δ) surface. The images were taken with different incident light intensities, 1.3×10^{18} cm^{-2} s^{-1} [$\sim$5 Suns, Fig. 4(a)] and 2.5×10^{16} cm^{-2} s^{-1} [$\sim$0.1 Suns, Fig. 4(b)], respectively. The letters "UNSW" were laser written into the front surface of the wafer using a laser process that is commonly used for writing the contact grooves into buried contact solar cells, but without the laser damage etch process that is usually applied subsequently in buried contact solar cell processing.

Both images in Fig. 4 clearly show the detrimental effect of the laser pattern on the local material quality (note that the color scale is different for the two measurements). With high incident light intensity [Fig. 4(a)] the contrast between the laser-damaged areas and the unaffected good quality regions is much sharper than in the low intensity measurement, where the laser damage appears as a featureless blurred area with strongly reduced PL intensity. These observations are explained by lateral current flow from good quality regions into bad quality regions, which are resistively connected in parallel to each other via the emitter.[17] Higher lateral currents at high light intensities cause higher resistive losses within the emitter. Consequently, higher light intensities yield higher contrast. In cases where lateral transport via an emitter or metal contacts occurs, these currents must be taken into account analytically in order to get the spatially resolved effective lifetime as demonstrated by Goldschmidt *et al.*[17] In this context it must be mentioned that in EL imaging on finished solar cells as reported by Fuyuki *et al.*,[15,16] the spa-
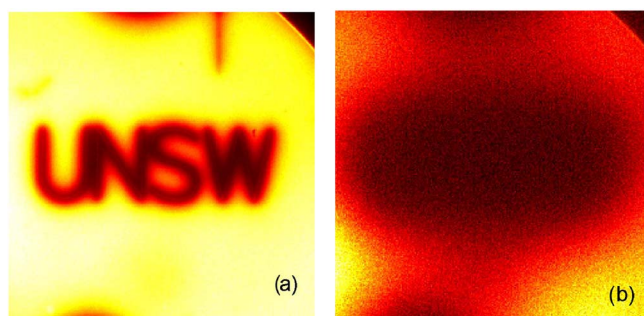
FIG. 4. (Color online) PL image (3.4×3.4 cm^2) of a monocrystalline silicon wafer which has locally been damaged by a laser, measured with (a) 13×10^{17} cm^{-2} s^{-1} ($\sim$5 Suns) and (b) 2.5×10^{16} cm^{-2} s^{-1} (0.1 Suns).

tial contrast that is observed can, to a large extent, be the result of such lateral series resistance losses caused by majority carrier transport.[18] PL imaging is advantageous in this regard, as it can be carried out on samples that are prepared without an emitter, in which the lateral equilibration via majority carrier transport does not occur. Three additional features appear in the image from Fig. 4(a). Two rounded low quality areas at the top and at the bottom of the sample result from one of several processing induced defects that have been identified at UNSW with PL imaging.[19,20] In addition, a crack in the wafer is clearly identified with PL imaging, a possibility that is important for photovoltaic manufacturing.

The high sensitivity of PL measurements also allows PL images to be taken at lower incident light intensities. A series of PL images taken with a range of different light intensities allows the spatially resolved injection level dependent effective lifetime to be measured. Measurements at the equivalent of 0.001 Suns have already been carried out on multicrystalline wafers in our laboratory.[21] Such measurements with variable light intensity will allow local *I*-*V* curves to be determined in analogy to the recently introduced Suns-photoluminescence technique[7] and local shunts within the wafer to be identified. The high sensitivity of PL is very beneficial in this context as it allows such measurements to be performed with reasonable data acquisition times. To avoid the influence on such measurements of lateral current flow especially at low light intensities as discussed above (Fig. 4), such measurements are ideally carried out on samples prior to the emitter diffusion. In that case lateral smearing of the contrast only occurs via minority carrier diffusion, which is expected to have only a marginal effect, as diffusion lengths in typical photovoltaic grade silicon wafers are on the same order of magnitude as the spatial resolution per pixel, i.e., a few hundred micrometers.

We have demonstrated PL imaging measurements on a large (8.5×8.5 cm^2) photovoltaic grade mc-Si wafer with very good (130 μm) spatial resolution, with a data acquisition time of only 1.5 s. Optimization of the measurement system, currently in progress in our laboratory, will allow significant increase in the system sensitivity by at least one order of magnitude. Industrial applications involving poorer quality wafers with lifetimes of only a few microseconds are thus also possible with data acquisition times of $\sim$1 s and reasonable spatial resolution. The fact that PL is contactless may even allow PL imaging to be used for *in situ* monitoring, e.g., for the optimization of processing steps such as the plasma-enhanced chemical-vapor deposition (PECVD) of SiN films or of thermal cycles such as the firing of screen printed metal contacts. Further practical advantages of PL imaging are the significantly lower cost of the CCD camera compared to the infrared cameras used for infrared absorption/emission imaging techniques, the fact that PL imaging can be performed with the sample at room temperature, that it can easily be performed on textured samples, and that it can be performed on finished devices with fully metallized rear surface.

In summary, PL imaging is a very promising, versatile, and fast experimental technique that provides insight into the spatial quality of silicon wafers without being affected by minority carrier trapping, by the DRM effect, or by temperature variations upon illumination. With these features we are confident that it will find wide applications in research and also in the photovoltaic and microelectronic industries.

[1] T. Trupke and R. A. Bardos, Proceedings of the 31st IEEE Photovoltaic Specialists Conference, Orlando, FL, 2005.

[2] P. J. Cousins, D. H. Neuhaus, and J. E. Cotter, J. Appl. Phys. **95**, 1854 (2004).

[3] M. Bail, M. Schulz, and R. Brendel, Appl. Phys. Lett. **82**, 757 (2003).

[4] R. A. Bardos, T. Trupke, M. C. Schubert, and T. Roth, Appl. Phys. Lett. **88**, 053504 (2006).

[5] R. A. Sinton, A. Cuevas, and M. Stuckings, Proceedings of the 25th IEEE Photovoltaic Specialists Conference, Washington, 1996.

[6] T. Trupke and R. A. Bardos, Proceedings of the 15th Crystalline Silicon Workshop, Vail, CO, August 2005.

[7] T. Trupke, R. A. Bardos, M. D. Abbott, and J. E. Cotter, Appl. Phys. Lett. **87**, 093503 (2005).

[8] S. Ostapenko, I. Tarasov, J. P. Kalejs, C. Haessler, and E. U. Reisner, Semicond. Sci. Technol. **15**, 840 (2000).

[9] E. Daub, P. Klopp, S. Kugler, and P. Würfel, Proceedings of the 12th EPVSC, Amsterdam, Netherlands, 1994.

[10] M. Bail, J. Kentsch, R. Brendel, and M. Schulz, Proceedings of the 28th IEEE Photovoltaic Specialists Conference, Anchorage, Alaska, 2000.

[11] S. Riepe, J. Isenberg, C. Ballif, S. W. Glunz, and W. Warta, Proceedings of the 17th EPVSC, Munich, Germany, 2001.

[12] M. C. Schubert, J. Isenberg, and W. Warta, J. Appl. Phys. **94**, 4139 (2003).

[13] P. Pohl, J. Schmidt, K. Bothe, and R. Brendel, Appl. Phys. Lett. **87**, 142104 (2005).

[14] M. C. Schubert, J. Isenberg, S. Rein, S. Bermejo, S. W. Glunz, and W. Warta, Proceedings of the 20th EPVSC, Barcelona, Spain, 2005.

[15] T. Fuyuki, H. Kondo, Y. Kaji, T. Yamazaki, Y. Takahashi, and Y. Uraoka, Proceedings of the 31st IEEE Photovoltaic Specialists Conference, Orlando, FL, 2005.

[16] T. Fuyuki, H. Kondo, T. Yamazaki, Y. Takahashi, and Y. Uraoka, Appl. Phys. Lett. **86**, 262108 (2005).

[17] J. C. Goldschmidt, O. Schultz, and S. W. Glunz, Proceedings of the 20th EPVSC, Barcelona, Spain, 2005, p. 663.

[18] T. Trupke, R. A. Bardos, M. D. Abbott, F. W. Chen, J. E. Cotter, and A. Lorenz, Proceedings of the WCPEC-4, Waikoloa, Hawaii, May 2006.

[19] F. W. Chen, J. E. Cotter, T. Trupke, and R. A. Bardos, Proceedings of the WCPEC-4, Waikoloa, Hawaii, May 2006.

[20] M. D. Abbott, J. E. Cotter, T. Trupke, K. Fischer, and R. A. Bardos, Proceedings of the WCPEC-4, Waikoloa, Hawaii, May 2006.

[21] Unpublished.